HgS quantum shells as a solution-processable gain material in the SWIR region

Korneel Molkens,[1,2] Dulanjan Harankahage[3,4], Jan Matthys[1], Dries Van Thourhout,[2] Mikhail Zamkov[3,4] and Pieter Geiregat[1]

[1] Physics and Chemistry of Nanostructures, Ghent University, Gent 9000, Belgium
[2] Photonics Research Group, Ghent University, Gent 9000, Belgium
3 The Center for Photochemical Sciences, Bowling Green State University, Bowling Green, Ohio 43403, United States
[4] Department of Physics, Bowling Green State University, Bowling Green, Ohio 43403, United States

Photonics is in a constant search of new gain materials to cover the broad wavelength range that applications need. This makes colloidal nanoparticles an interesting class of materials due to their tunable bandgap, solution processability and stability as an inorganic material [1]. A good infrared colloidal emitter, however, is not readily available. In this work, we characterize a new material that bridges this gap: HgS quantum shells, similar to CdSe quantum shells reported earlier [5]. The material consists of a CdS core, with a low bandgap HgS shell around it, creating a curled-up quantum well. We show an intrinsic gain of 1200 cm^{-1} in the wavelength range between 1030 and 1150 nm via transient absorption spectroscopy. The gain threshold is $8.5 \cdot 10^{12}$ cm^{-2} and is understood by simulating the occupation of the energy levels. We also show that the carriers recombination rate scales with the carrier density, limiting the gain lifetime at higher carrier densities to the 100 ps range. Our results show that this material is a first step in the creation of colloidal quantum shells in the near-infrared wavelength range

Introduction

With the commercialization of QLED displays, colloidal nanocrystal technology reached a high maturity level. Due to their versatility and cheap fabrication, it is likely that they will find applications outside display technology, for example as gain material in integrated photonics. The field of integrated photonics has been in a search for a good gain material for many decades, and nanocrystals in various forms have shown potential [1] [2]. These reports focus on materials that emit in the visible wavelength range. The infrared wavelength range however, is technologically relevant but there are little reports on colloidal gain materials [3].

Mercury chalcogenide (HgX) nanocrystals are potential gain materials in this wavelength range. Their semi-metallic character makes their emission tunable over the full infrared wavelength range [3]. HgTe have shown gain before [4]. The gain magnitude however, is limited to 100 – 500 cm^{-1}. Recently, a large gain magnitude was shown in an alternative nanocrystal architecture in the visible range with colloidal quantum shells (CQS) [5]. This works investigates the possibility of using this architecture for HgS that emits in the infrared.

The study starts with the calculation of the energy levels and density of states (DOS) in a CQS structure. The DOS is then used to calculate the gain threshold carrier density. To experimentally verify these results, we use transient absorption (TA) spectroscopy. TA also yields the carrier dynamics, revealing an second-order recombination process.

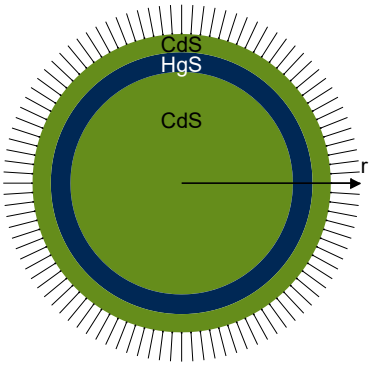

Figure 1. Architecture of a colloidal CdS/HgS/CdS quantum shell.

Calculation of the gain threshold carrier density

The QS confine the electrons in all three spatial dimensions. Hence, the DOS is given by a discrete summation of the different energy levels. Given the particular morphology of the nanocrystal, the position of these energy levels is not readily obtained via Brus' equation. Therefore, Schrödinger's equation is solved in an effective mass approximation as outlined by Schooss et al [6]. In short, the wavefunction is separated into a radial and angular part. The angular part is given by spherical harmonics, due to the radial symmetry. The radial part consists of a combination of spherical Bessel functions. The resulting wavefunction of the lowest energy level of the electrons and the holes is given in figure 2a.

The solutions are distinguished by three quantum numbers. The principal quantum number n will always be 1, since the shell is very thin compared to the electron wavelength in HgS. The angular quantum numbers l and m will respectively determine the energy and degeneracy of each solution. Figure 2b shows the solutions for different l's and m's. Each l yields a different energy (E_l) while the degeneracy is given by $g_l = 2l + 1$. The DOS is given by a sum over all these energy levels:

$$DOS_n(E) = \frac{1}{A_{shell}} g_n \sum_l g_l \delta(E - E_l) \tag{1}$$

The factor g_n is the degeneracy in the bulk band diagram (2-fold for electrons, 8-fold for holes [3]). We divide by the shell area, to obtain the unit of cm^{-2}. The electron density in a semiconductor follows the Fermi-Dirac distribution. The total electron density is an integral over this distribution, and the DOS.

$$n(E_{F,n}) = \int_{E_c}^{+\infty} DOS(E) f\big(E; E_{F,n}, T\big) dE \tag{2}$$

Combing equations (1) and (2) results in

$$n(E_{F,n}) = \frac{2G_n}{A_{shell}} \sum_l \frac{1}{e^{\frac{E_l - E_{F,n}}{kT}} + 1}$$

This expression relates the carrier density with the position of the electron quasi Fermi level. A similar expression for the holes allows to calculate the hole quasi Fermi level. According to the Bernard-Duraffourg condition, the spacing between these quasi Fermi levels should exceed the bandgap to obtain optical gain. The bandgap is then the sum of the bulk bandgap and the confinement energy. This allows us to calculate an estimation of the transparency carrier density of the first transition as $8.5 \cdot 10^{12}$ cm^{-2}.

Charge densities above the gain threshold will shift the quasi Fermi levels even further into the conduction and valence band, increasing the photon energy at which gain is achieved. Figure 2d shows the dependency of the quasi Fermi level separation on the injected charge density, together with the experimental results that are described in the next section.

Transient absorption measurements

To experimentally quantify the gain, we performed linear and transient absorption measurements. The linear absorption is shown in figure 2b. The curves has a gradual and featureless increase towards the CdS bandgap around 2.25 eV. The featurelessness confirms the close proximity of the different electron states, unlike quantum dots. The increase with energy confirms the raising DOS, unlike nanoplatelets where this is flat. Finally, no exciton formation is visible. We attribute this to shielding of the Coulomb interaction due to the

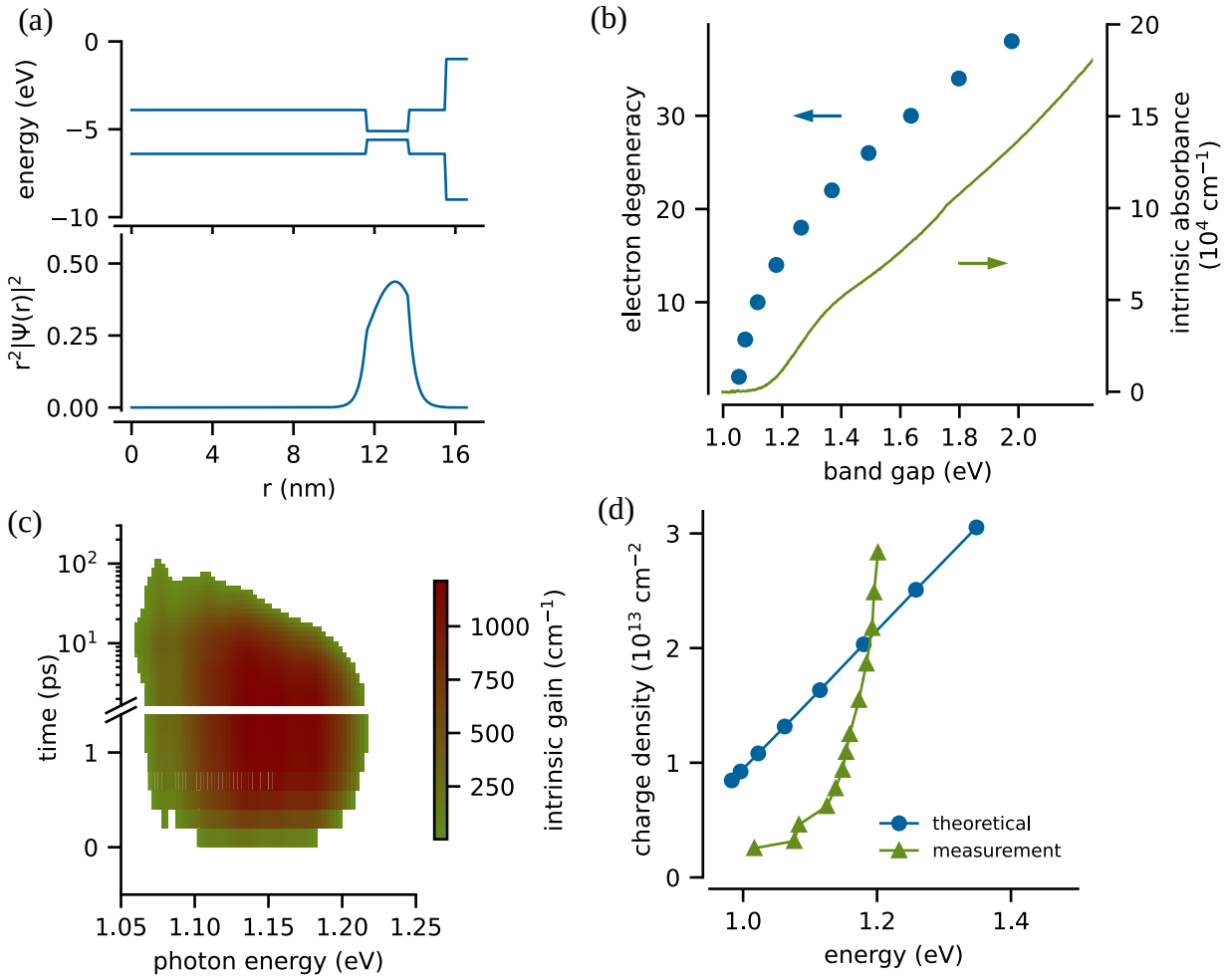

Figure 2: (a) The bulk band structure (top) and the wavefunction of the lowest energy electon wavefuntion (bottom). (b) The energy and degeneracy of the different solutions, together with the absorption spectrum. (c) Gain map obtained via TA measurements (d) highest photon energy for which the sample is not absorbing, for different charge densities.

presence of CdS [7] and the low effective mass for both electrons and holes in HgS [6], yielding a low exciton binding energy.

Transient absorption measurements are performed by optically exciting the sample with a 800 nm pump pulse and measuring the change of absorption with a second broadband probe pulse. The probe is delayed from the pump via a delay stage, and spectrally resolved with a spectrometer. The total absorption after optical excitation is obtained by adding the transient absorption to the linear absorption. If the total absorption is negative, the sample amplifies light, instead of absorbing it. Figure 2c shows the gain map of our sample at the highest pump fluence. The gain spans a range of more than 100 nm (1030 to 1150 nm) and has a lifetime around 100 ps (see below).

This measurement was repeated for different pump fluences. For each fluence, we calculated the charge density in the shell, and the highest photon energy for which there is gain. This is shown in figure 2d, together with the highest energy of inversion that is described in the previous section. The two graphs show a similar order of magnitude for the transparency carrier density. It should be noted that there is uncertainty in both the theoretical as experimental parameters.

The gain lifetime is limited to the 100 ps range. To investigate this further, figure 3 shows the decay in transient absorption, which is proportional to the carrier density. We performed global fitting to this data, keeping the same decay rate for every trace. The best fit is obtained for a n^2-decay process. The decay of carrier density is than proportional to the square of the carrier density:

$$\frac{dn}{dt} = k_2 n^2 \Rightarrow n(t) = \frac{1}{A + k_2 t}$$

In literature, the n^2-decay has been attributed to exciton-exciton annihilation [8], or an carrier density-dependent stimulated emission rate [5].

Conclusion

In this study, we determined the gain threshold carrier density both theoretically and experimentally, and found a good match between the two. The method can be applied to a broad range of nanocrystals, specifically those who are weakly confined. This allows for the engineering of new nanomaterials to achieve low gain thresholds.

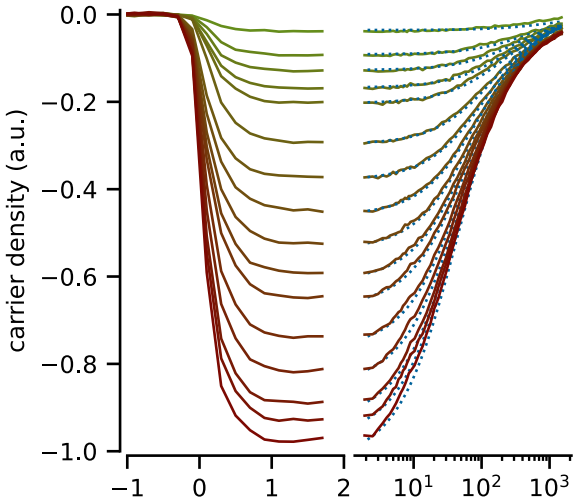

Figure 3. Decay of transient absorption integrated between 850 and 110 nm, for increasing excitation density. The fit is shown as a blue dashed line.

Bibliography

[1] N. Ahn *et al.*, "Electrically driven amplified spontaneous emission from colloidal quantum dots," *Nature*, vol. 617, no. 7959, pp. 79–85, May 2023, doi: 10.1038/s41586-023-05855-6.

[2] W. Xie *et al.*, "On-Chip Integrated Quantum-Dot–Silicon-Nitride Microdisk Lasers," *Adv. Mater.*, vol. 29, no. 16, p. 1604866, 2017, doi: 10.1002/adma.201604866.

[3] C. Gréboval, A. Chu, N. Goubet, C. Livache, S. Ithurria, and E. Lhuillier, "Mercury Chalcogenide Quantum Dots: Material Perspective for Device Integration," *Chem. Rev.*, vol. 121, no. 7, pp. 3627–3700, Apr. 2021, doi: 10.1021/acs.chemrev.0c01120.

[4] P. Geiregat *et al.*, "Continuous-wave infrared optical gain and amplified spontaneous emission at ultralow threshold by colloidal HgTe quantum dots," *Nat. Mater.*, vol. 17, no. 1, pp. 35–42, Jan. 2018, doi: 10.1038/nmat5000.

[5] I. Tanghe *et al.*, "Two-Dimensional Electron–Hole Plasma in Colloidal Quantum Shells Enables Integrated Lasing Continuously Tunable in the Red Spectrum," *ACS Nano*, vol. 18, no. 22, pp. 14661–14671, Jun. 2024, doi: 10.1021/acsnano.4c02907.

[6] D. Schooss, A. Mews, A. Eychmüller, and H. Weller, "Quantum-dot quantum well CdS/HgS/CdS: Theory and experiment," *Phys. Rev. B*, vol. 49, no. 24, pp. 17072–17078, Jun. 1994, doi: 10.1103/PhysRevB.49.17072.

[7] J. J. Geuchies *et al.*, "Zero-Threshold Optical Gain in Electrochemically Doped Nanoplatelets and the Physics Behind It," *ACS Nano*, vol. 16, no. 11, pp. 18777–18788, Nov. 2022, doi: 10.1021/acsnano.2c07519.

[8] D. Sun *et al.*, "Observation of Rapid Exciton–Exciton Annihilation in Monolayer Molybdenum Disulfide," *Nano Lett.*, vol. 14, no. 10, pp. 5625–5629, Oct. 2014, doi: 10.1021/nl5021975.